Context-Aware Single Image Rain Removal

De-An Huang[1,2], Li-Wei Kang[3], Min-Chun Yang[1,4], Chia-Wen Lin[5], and Yu-Chiang Frank Wang[1]

[1]Research Center for Information Technology Innovation, Academia Sinica, Taipei, Taiwan
[2]Department of Electrical Engineering, National Taiwan University, Taipei, Taiwan
[3]Institute of Information Science, Academia Sinica, Taipei, Taiwan
[4]Department of Computer Science and Information Engineering, National Taiwan University, Taipei, Taiwan
[5]Department of Electrical Engineering, National Tsing Hua University, Hsinchu, Taiwan
[1]ycwang@citi.sinica.edu.tw, {[2]b97901010, [4]d96922009}@ntu.edu.tw, [3]lwkang@iis.sinica.edu.tw, [5]cwlin@ee.nthu.edu.tw

***Abstract*—Rain removal from a single image is one of the challenging image denoising problems. In this paper, we present a learning-based framework for single image rain removal, which focuses on the learning of context information from an input image, and thus the rain patterns present in it can be automatically identified and removed. We approach the single image rain removal problem as the integration of image decomposition and self-learning processes. More precisely, our method first performs context-constrained image segmentation on the input image, and we learn dictionaries for the high-frequency components in different context categories via sparse coding for reconstruction purposes. For image regions with rain streaks, dictionaries of distinct context categories will share common atoms which correspond to the rain patterns. By utilizing PCA and SVM classifiers on the learned dictionaries, our framework aims at automatically identifying the common rain patterns present in them, and thus we can remove rain streaks as particular high-frequency components from the input image. Different from prior works on rain removal from images/videos which require image priors or training image data from multiple frames, our proposed self-learning approach only requires the input image itself, which would save much pre-training effort. Experimental results demonstrate the subjective and objective visual quality improvement with our proposed method.**

Keywords-rain removal; sparse coding; dictionary learning; self-learning; image decomposition

I. INTRODUCTION

Different weather conditions such as rain, snow, or haze will cause complex visual effects on spatial or temporal domains in images or videos [1]-[7]. Such effects may significantly degrade the quality or performance of vision systems relying on image/video feature extraction [8] or visual attention modeling [9] such as object detection, tracking, and recognition. Among image denoising problems, rain removal has recently received the attention from researchers [1]-[7]. While most of the existing approaches are based on the detection and removal of rain streaks in a video [1]-[6], a recently proposed method focuses on single image rain removal [7], which advocates the use of morphological component analysis (MCA) [10] with possible use of training image data to identify rain patterns in the input image. For completeness, we briefly review current image/video-based rain removal approaches, followed by presenting the contributions of the proposed method.

A. Video-based Rain Detection and Removal

A pioneering work on detecting and removing rain streaks in a video was proposed in [1], in which a correlation model capturing the dynamics of rain and a physics-based motion blur model characterizing the photometry of rain were developed. It was subsequently shown in [2] that some camera parameters such as exposure time and depth of field can be selected to mitigate the effects of rain without altering the appearance of the scene. Furthermore, how to model the shape and appearance of a single rain or snow streak in the image space was studied in [5]. As a result, the amount of rain or snow in videos can be altered. In [6], selection rules based on photometry and size were proposed to detect the potential rain streaks in a video by calculating the histogram of orientations of rain streaks with geometric moments.

Current video-based approaches may suffer from some practical scenarios described as follows. For removing rain streaks from videos acquired from a moving camera, the performance of existing approaches may be significantly degraded due to the non-stationary background (by camera motion or inaccurate motion estimation). Moreover, for the case of steady effects of rain, i.e., pixels may be affected by rain across multiple consecutive frames, it is difficult to detect such pixels or find reliable information from neighboring frames to recover them [1]. Furthermore, some video-based approaches [2] based on adjusting camera parameters may not be suitable to consumer camcorders and cannot be applied to existing acquired image/video data.

In addition, when only a single image is available, such as an image captured from a camera-phone or downloaded from the Internet, a rain removal approach based on a single input image is needed. Many image-based applications such as mobile visual search and object detection/recognition heavily rely on extraction of gradient-based features (e.g., histogram of oriented gradients (HOG) [8]). Their performance can be remarkably degraded by rain streaks present in an image due to additional gradients introduced by rain streaks. Furthermore, while visual attention models [9] compute a saliency map, which is topographically encoding for saliency at each pixel location, their performance might also be degraded if rain streaks directly interact with the target/region of interest in an image. Therefore, a rain removal approach based on a single image is highly desirable.

B. Single Image Rain Removal

Recently, a single-image rain removal approach was proposed in [7], which approaches the rain removal task as the image decomposition problem based on MCA [10]. Instead of directly applying conventional image decomposition techniques, it first

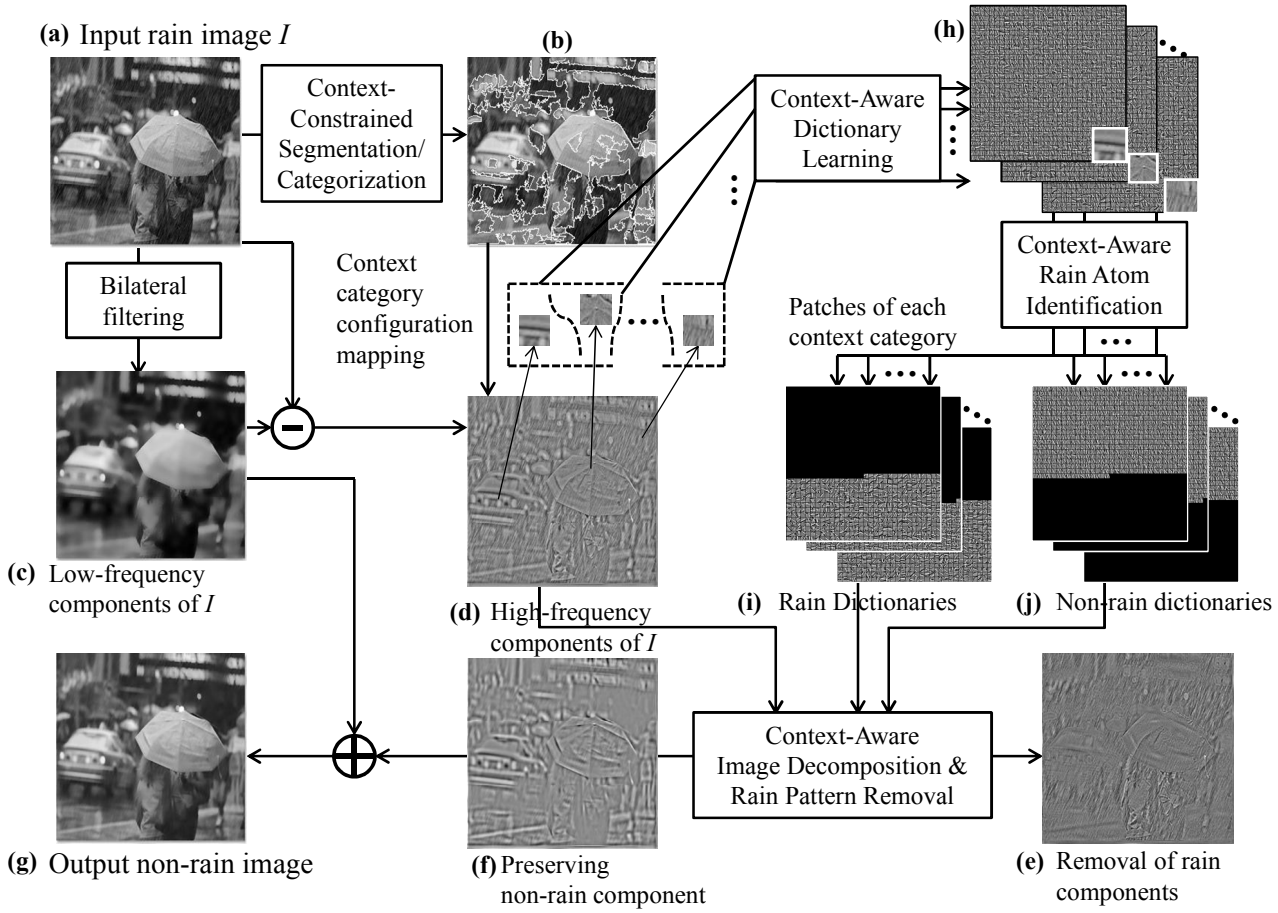

Figure 1. Block diagram of the proposed method for single image rain removal.

separates a rain image into low and high-frequency parts using a bilateral filter [11]. The high-frequency ones are then decomposed into a set of "rain components" and the other with "non-rain components" by performing K-means clustering (K = 2) on the associated dictionary in terms of HOG features (with possible use of training data). While very promising results were reported in [7], dividing image atoms into two distinct groups using HOG features does not guarantee accurate classification between rain and non-rain patterns. Therefore, a more robust method is needed to further improve the performance.

C. Our Contributions

To design a more reliable approach for single image rain removal, as illustrated in Figure 1, we propose a framework which learns context information in an unsupervised setting, while the rain patterns can be automatically identified and removed from dictionaries learned for each context category. Different from prior rain removal methods, we not only approach this problem as the estimation/detection of rain patterns from the input image, we aim at designing an *image and context-dependent* rain removal framework without the need to utilize any training image data or the assumptions on any image priors. The major contribution of this paper is three-fold: (i) by performing context-aware dictionary learning, the rain/non-rain atoms for each context category can be learned adaptively and automatically; (ii) the proposed rain removal process for each context category is performed independently, which can be processed in parallel for speedup; and (iii) the learning of dictionaries for image decomposition and reconstruction is fully automatic, self-contained, and adapted to different types of images.

The rest of this paper is organized as follows. In Section II, we briefly review the concepts of MCA-based image decomposition via dictionary learning and sparse coding, and the technique of context-constrained image segmentation and categorization. Section III presents the proposed framework for single image rain removal. Experimental results and comparisons are presented in Section IV, and Section V concludes this paper.

II. Related Works

A. MCA-based Image Decomposition via Dictionary Learning and Sparse Coding

We now briefly discuss how morphological component analysis (MCA) [10] is applied for image decomposition using of dictionary learning and sparse coding techniques. Suppose that an image I of N pixels is a superposition of S layers (called morphological components), denoted by $I = \sum_{s=1}^{S} I_s$, where I_s denotes the s-th component, such as the geometric or textural component of I. To decompose the image I into $\{I_s\}_{s=1}^{S}$, MCA iteratively minimizes the following energy function:

$$E(\{I_s\}_{s=1}^{S}, \{\theta_s\}_{s=1}^{S}) = \frac{1}{2}\left\| I - \sum_{s=1}^{S} I_s \right\|_2^2 + \tau \sum_{s=1}^{S} E_s(I_s, \theta_s), \quad (1)$$

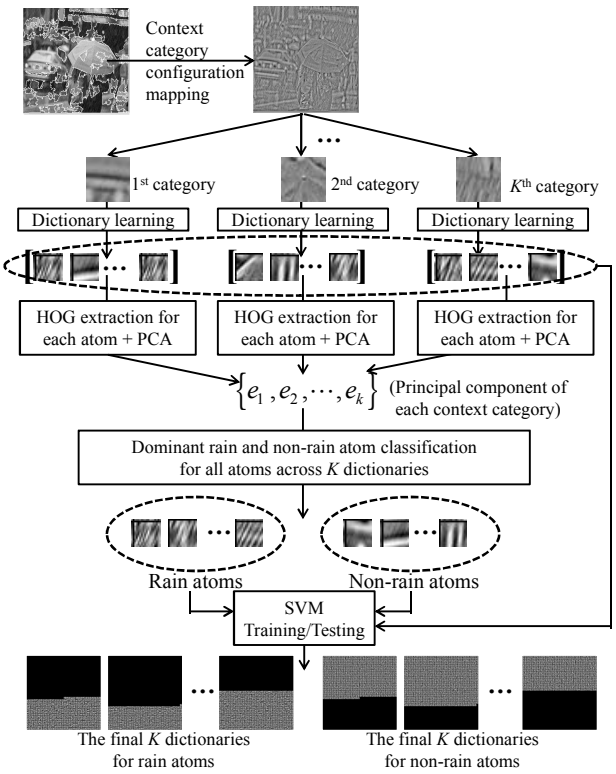

Figure 2. Block diagram of the proposed context-aware dictionary learning for rain/non-rain pattern identification.

where θ_s denotes the sparse coefficients corresponding to I_s with respect to dictionary D_s, τ is a regularization parameter, and E_s is the energy defined according to the type of D_s (global or local dictionary). The MCA algorithm solves (1) by iteratively performing the following two steps: (i) perform sparse coding to solve θ_s or $\{\theta_s^p\}_{p=1}^N$, where θ_s^p represents the sparse coefficients of patch b_s^p extracted from I_s, to minimize $E_s(I_s, \theta_s)$ while fixing I_s; and (ii) update I_s or $\{b_s^p\}_{p=1}^N$ while fixing θ_s or $\{\theta_s^p\}_{p=1}^N$.

To construct a dictionary D_s for sparsely representing each patch b_s^p extracted from the component I_s of the image I, one may use a set of available training exemplars $y^p, p = 1,2,\dots,P$, to learn a dictionary D_s, and solve the following optimization problem:

$$\min_{D_s,\theta^p} \sum_{p=1}^{P} \left(\frac{1}{2} \|y^p - D_s\theta^p\|_2^2 + \lambda \|\theta^p\|_1 \right), \qquad (2)$$

where θ^p denotes the sparse coefficients of y^p with respect to D_s and λ is a regularization parameter. Equation (2) can be efficiently solved by performing a dictionary learning algorithm, such as the online dictionary learning algorithm [12], where the sparse coding step is usually achieved via OMP (orthogonal matching pursuit). Finally, the image decomposition is achieved by iteratively performing MCA to solve I_s (while fixing D_s) and the dictionary learning algorithm to learn D_s (while fixing I_s) until convergence.

In this paper, we extend the framework of [7] and approach the single image rain removal problem as the integration of image decomposition and self-learning processes. As will be elaborated later in Section III, our proposed framework combines context-aware image decomposition by MCA and self-learning (via PCA and SVM) to automatically identify/remove rain patterns from the input image.

B. Context-constrained Image Segmentation and Categorization

The context-constrained image segmentation and categorization technique was first developed in [13] for image super-resolution purposes. In our rain removal framework, we first apply this technique to a rain image and divide the image into patches with different context categories. As suggested in [13], we apply the mean-shift algorithm [14] to over-segment the input image into several segments (i.e., *superpixels*). Each segment can be automatically categorized into different groups according to their textural features via affinity propagation (AP) algorithm [15], which is an unsupervised clustering algorithm which groups the data by identifying the exemplars of each cluster. The major advantage of AP is that, unlike other clustering algorithms such as *K*-means, it does not need the number of clusters *K* as prior knowledge. Therefore, the use of AP allows us to automatically categorize the image segments into different context categories, and no user interaction or parameter tuning is needed.

III. THE PROPOSED RAIN REMOVAL FRAMEWORK

Figure 1 shows our framework for single image rain removal framework, which approaches the single image rain removal problem as decomposing the input image and learning context-aware rain/non-rain patterns. We now detail the proposed method.

A. Context-aware Image Decomposition and Dictionary Learning

In the preprocessing step, an input rain image I in Figure 1(a) is first divided into K context categories I^k, k = 1, 2, …, K, where $I = \bigcup_{k=1}^{K} I^k$ is produced by the technique of context-constrained image segmentation and categorization, as shown in Figure 1(b) and discussed in Section II.B. Meanwhile, as illustrated in Figure 1(c) and (d), the input image I is decomposed into the low-frequency (LF) part I_{LF} and the high-frequency (HF) part I_{HF} using bilateral filtering [11], where the strength of smoothness of the bilateral filter is adjusted such that almost all of the rain streaks are retained in I_{HF} whereas I_{LF} contains negligible amount of rain streaks. Once this preprocessing process is complete, we map the derived context-constrained categorization configuration for I into I_{HF}, i.e., we assign the resulting context labels to I_{HF} and have I_{HF}^k, k = 1, 2, …, K, where $I_{HF} = \bigcup_{k=1}^{K} I_{HF}^k$. In other words, each superpixel in I_{HF} has an associated context label, and thus we successfully extract HF superpixels with their context information.

Next, our method learns a dictionary D_{HF}^k for the context category I_{HF}^k based on the training exemplar patches extracted from I_{HF}^k for reconstruction purposes. Our ultimate goal is to separate the dictionary D_{HF}^k for context category k into two sub-dictionaries $D_{HF\_R}^k$ and $D_{HF\_G}^k$, which represent the rain and geometric (non-rain) components of the HF part I_{HF}^k, respectively. As a result, we formulate the problem of rain removal for the context category k as a sparse coding-based image decomposition problem as follows:

$$\left(\theta_{HF}^{k\_p}\right)^* = \arg\min_{\theta_{HF}^{k\_p}} \left(\frac{1}{2} \left\| b_{HF}^{k\_p} - D_{HF}^k \theta_{HF}^{k\_p} \right\|_2^2 + \lambda \left\| \theta_{HF}^{k\_p} \right\|_1 \right), \qquad (3)$$

where $b_{HF}^{k\_p} \in \mathrm{R}^n$ represents the p-th patch extracted from I_{HF}^k, $p = 1,2,\dots,P$. $\theta_{HF}^{k\_p} \in \mathrm{R}^m$ represents the vector of sparse coefficients of $b_{HF}^{k\_p}$ with respect to $D_{HF}^k \in \mathrm{R}^{n\times m}, n \le m$, λ is a regularization parameter, and $\left(\theta_{HF}^{k\_p}\right)^*$ denotes the solution to (3). We apply sparse coding techniques for image representation and reconstruction, since it has proven to be an effective tool in many image-related applications [15]. To solve (3), we apply the efficient OMP

algorithm provided by [12]. Each patch $b_{HF}^{k\_p}$ can be reconstructed and used to recover either the geometric or the rain component of I_{HF}^{k} depending on the corresponding nonzero coefficients in $\left(\theta_{HF}^{k\_p}\right)^{*}$, i.e., the used atoms from $D_{HF\_G}^{k}$ or $D_{HF\_R}^{k}$.

As shown in Figure 1(h), once the dictionaries for HF image components of different context categories are learned, we will focus on the identification of rain and non-rain atoms from these dictionaries (see Figures 1(f) and 1(e), respectively). As a result, together with the LF parts of the input image, these non-rain patterns can be applied to recover the original image without the presence of rain streaks. In the following subsections, we will discuss how our method automatically divides the dictionary atoms of different context categories into rain and non-rain patterns.

In the image decomposition step, for each context category, a dictionary learned from the training exemplars extracted from the corresponding regions in the HF part of the image itself can be used to generate two sub-dictionaries (rain and non-rain dictionary) via dominant rain streak direction identification using PCA [16] and SVM clustering [17]. Then, we perform sparse coding [12] based on the two sub-dictionaries to achieve MCA-based image decomposition individually for each context category, where the geometric component in the HF part can be obtained, followed by integrating with the LF part of the image to obtain the rain-removed version of this image, as illustrated in Figure 1(g). The detailed method shall be elaborated below.

B. Automatic Identification of Rain/non-rain Atoms

In order to separate the dictionary atoms of D_{HF}^{k} into two distinct clusters (sub-dictionaries), one representing the rain patterns and the other for geometric (non-rain) patterns, we need to develop an automatic approach to perform the above clustering problem in an unsupervised way. In [7], the atoms in a learned dictionary for an image was divided into two sub-dictionaries using the *K*-means clustering (K = 2) based on the associated HOG [8] features. However, the approach in [7] did not utilize any image or context-specific information when learning the dictionary. Moreover, performing a hard-clustering like *K*-means clustering based on HOG features does not guarantee accurate separation of dictionary atoms into rain and non-rain patterns. Therefore, one of the major contributions of our proposed framework is to exploit the local characteristics of context categories further improve the method of [7], so that we can achieve quantitatively and qualitatively better performance than that of [7].

In our method, instead of learning only one dictionary for an image in [7], we propose to learn the dictionary D_{HF}^{k} for each context category (as discussed in Section III.A), followed by an automatic identification of atoms which correspond to rain and non-rain patterns. We observe that, in most rain images, the rain streaks are present in the entire image and with similar gradients. Therefore, the dictionaries learned from different context categories should share common atoms which indicate the rain patterns. On the other hand, for dictionary atoms which are strongly uncorrelated to each other across different context categories, they should be associated with geometric structure of the image and thus can be considered as non-rain patterns.

As illustrated in Figure 2, to find the rain atoms for an image, we first utilize the HOG descriptor to describe the gradient information of each atom d_i^k, i = 1, 2, …, N_k, in D_{HF}^{k}, where N_k is the number of atoms in D_{HF}^{k}, k = 1, 2, …, K. Next, we apply PCA [16] to determine the principal component for the atoms in each context category, i.e., the eigenvector with the largest eigenvalue for each D_{HF}^{k}. Consistent with our observations, we find that most principal components from different context categories are very similar to each other in rain images, and thus these principal components of rain streaks for the input image (described by a set of eigenvectors, e_k, k = 1, 2, …, K) can be used to identify the most similar/dissimilar atoms indicating rain/non-rain patterns. More specifically, based on the derived principal components e_k, k = 1, 2, …, K, we can extract the top N similar/dissimilar atoms d_i^k, i = 1, 2, …, N_k, k = 1, 2, …, K, into two clusters, one representing the rain patterns and the other indicating the non-rain ones, as shown in the middle of Figure 2.

After the above unsupervised clustering process is complete, we collect two sets of atoms which correspond to rain and non-rain atoms with high confidence, and we train a support vector machine (SVM) [17] classifier on them. This SVM classifier is used to classify the remaining atoms in the dictionaries D_{HF}^{k} (i.e., not the most similar or dissimilar ones to the principal components), so that the classifying/clustering results are totally image and context-dependent. Once this process is complete, we successfully and automatically classify all the atoms of the dictionary D_{HF}^{k} into rain sub-dictionary $D_{HF\_R}^{k}$ and non-rain sub-dictionary $D_{HF\_G}^{k}$, as illustrated in Figures 1(i) and 1(j), respectively. Finally, for each context category, we obtain a sub-dictionary pair for rain and non-rain patterns, and the former one will be disregarded during reconstruction for the purpose of rain removal.

C. Removal of Rain Streaks

We now discuss how we utilize the rain patterns identified in Section III.B to address rain removal. As shown in Figures 1 and 2, based on the two sub-dictionaries $D_{HF\_R}^{k}$ and $D_{HF\_G}^{k}$ for the k-th context category, we perform sparse coding and apply OMP for each image patch $b_{HF}^{k\_p}$ extracted from I_{HF}^{k} via minimization of (3), and we obtain its sparse representation $\left(\theta_{HF}^{k\_p}\right)^{*}$ with respect to $D_{HF}^{k} = \left[D_{HF\_R}^{k} | D_{HF\_G}^{k}\right]$. Now, each reconstructed patch $b_{HF}^{k\_p}$ can be used to recover either rain component $I_{HF\_R}^{k}$ or geometric component $I_{HF\_G}^{k}$ of I_{HF}^{k} based on the sparse coefficients $\left(\theta_{HF}^{k\_p}\right)^{*}$. More precisely, we set the coefficients corresponding to $D_{HF\_G}^{k}$ in $\left(\theta_{HF}^{k\_p}\right)^{*}$ to zeros to obtain $\left(\theta_{HF\_R}^{k\_p}\right)^{*}$, while the coefficients corresponding to $D_{HF\_R}^{k}$ in $\left(\theta_{HF}^{k\_p}\right)^{*}$ to zeros to obtain $\left(\theta_{HF\_G}^{k\_p}\right)^{*}$. Therefore, each patch $b_{HF}^{k\_p}$ can be re-expressed as either $b_{HF\_R}^{k\_p} = D_{HF\_R}^{k} \times \left(\theta_{HF\_R}^{k\_p}\right)^{*}$ or $b_{HF\_G}^{k\_p} = D_{HF\_G}^{k} \times \left(\theta_{HF\_G}^{k\_p}\right)^{*}$, which can be used to recover $I_{HF\_R}^{k}$ or $I_{HF\_G}^{k}$, respectively, by averaging the pixel values in overlapping regions. Finally, as shown in Figure 1(g), the rain-removed version of image I can be obtained via $I^{Non\_Rain} = I_{LF} + I_{HF\_G}$, where $I_{HF\_G} = \bigcup_{k=1}^{K} I_{HF\_G}^{k}$, i.e., integration of each individually rain-removed context category $I_{HF\_G}^{k}$, k = 1, 2, …, K.

TABLE I.

PERFORMANCE COMPARISONS (IN PSNR (DB)) USING BILATERAL FILTERING [11], THE K-SVD BASED IMAGE DENOISING METHOD [18], THE MCA-BASED METHOD [7], AND OUR PROPOSED METHOD.

	Bilateral [11]	**K-SVD based Denoising [18]**	**MCA-based [7]**	**Proposed**
Figure 3	20.08	20.90	21.02	**21.04**
Figure 4	19.00	19.46	19.49	**19.57**
Figure 5	23.85	24.17	24.13	**24.23**

IV. EXPERIMENTAL RESULTS

To evaluate the performance of the proposed algorithm, we compare the proposed method with bilateral filtering (denoted by

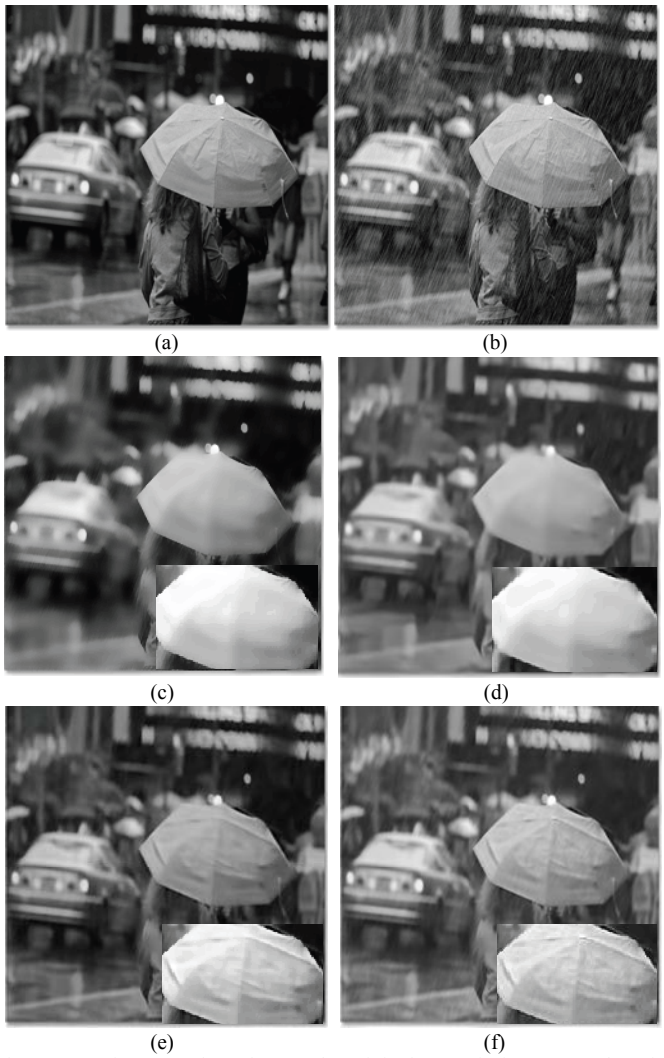

Figure 3. Rain removal results: **(a)** the original non-rain image; **(b)** the rain image of (a); the rain-removed versions of (b) via the: **(c)** bilateral filter; **(d)** K-SVD-based denoising method; **(e)** MCA-based method; and **(f)** proposed method.

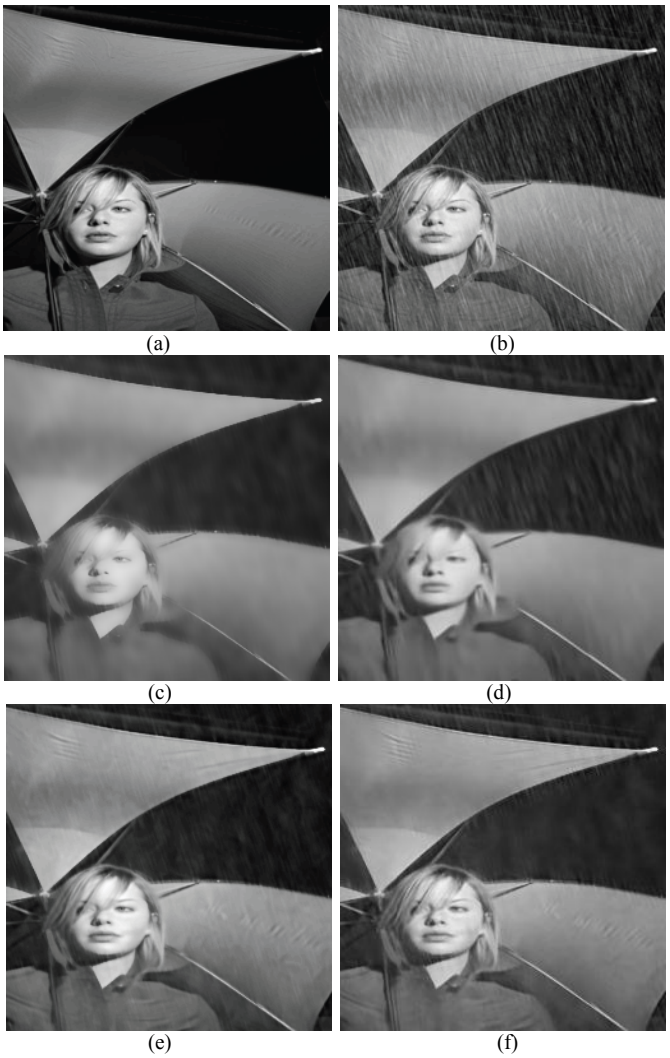

Figure 4. Rain removal results: **(a)** the original non-rain image; **(b)** the rain image of (a); the rain-removed versions of (b) via the: **(c)** bilateral filter; **(d)** *K*-SVD-based denoising method; **(e)** MCA-based method; and **(f)** proposed method.

"Bilateral") [11], the state-of-the-art image denoising method based on K-SVD dictionary learning and sparse representation (denoted by "K-SVD-based denoising") [18], and the first single-image-based rain removal method based on MCA (denoted by "MCA-based") [7]. We collect several synthetic rain images from the Internet or the photo-realistically rendered rain video frames provided in [3] (with ground-truth images). To evaluate the quality of a rain-removed image with ground-truth, we calculate the PSNR (peak signal-to-noise ratio) values for the resulting images.

The parameter settings for different methods are described as follows. The spatial-domain and intensity-domain standard deviations of the bilateral filter [11] were set to 6 and 0.2, respectively, for ensuring that most rain streaks in a rain image can be removed. In the dictionary learning step [12], the regularization parameter λ used in (2) was set to 0.15, as suggested by [12]. For each test gray-scale image of size 256×256, the patch size, dictionary size for each context category, and the number of training iterations are set to n = 16×16, m = 1024, and 100, respectively. The dimension of each HOG feature descriptor [8] was set to 81. The SVM classifier for dictionary classification and rain pattern identification was trained by LIBSVM [17].

Figures 3–5 compare the rain removal results obtained from bilateral filtering [11], the K-SVD method [18], the MCA-based method [7], and the proposed method. The PSNR results for the test images with ground-truths are listed in TABLE I. The experimental results demonstrate that although the bilateral filter and the K-SVD denoising method can remove most rain streaks, they simultaneously remove much image detail as well. Moreover, although the MCA-based method can well remove most rain streaks without significantly degrading image quality in most cases, parts of non-rain components may be also removed as well due to the heuristic dictionary partition. The proposed method successfully removes most rain streaks while preserving most non-rain image details in these test cases, thereby improving the subjective visual quality. For example, in Figure 3, more details in the umbrella (highlighted in the right bottom side in each figure) can be better recovered by our method. It can be also observed from TABLE I that the PSNR performance of the proposed method outperforms the existing methods used for comparisons. However, the PSNR performance gaps among the evaluated methods are usually insignificant because the PSNR metric cannot well reflect the visual quality of rain-removed images. Besides the visual quality

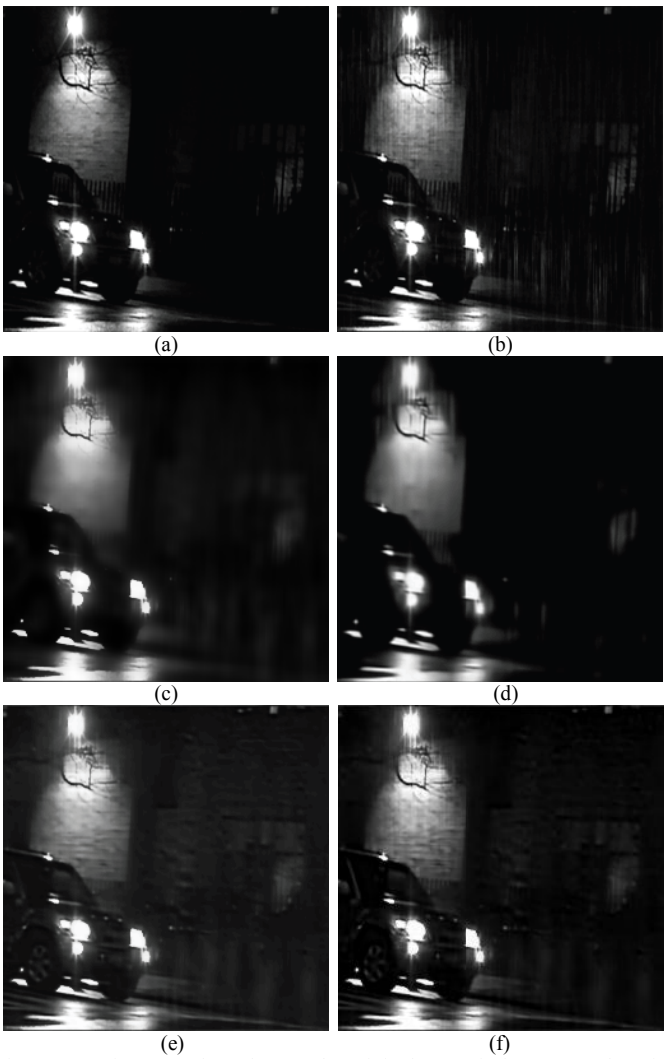

Figure 5. Rain removal results: **(a)** the original non-rain image; **(b)** the rain image of (a); the rain-removed versions of (b) via the: **(c)** bilateral filter; **(d)** K-SVD-based denoising method; **(e)** MCA-based method; and **(f)** proposed method.

improvement, another unique advantage of our method is that the context-aware processing manner can be easily realized in parallel, which is beneficial to real applications.

V. CONCLUSION

In this paper, we presented a context-aware single image rain removal method, which formulates the rain removal problem as a joint image decomposition and self-learning process. The proposed self-learning framework is able to extract image-specific context information, and thus the rain patterns present in the input image can be identified and removed automatically. By advancing the techniques of context-constrained image segmentation, categorization, and sparse coding, we learned dictionaries for high-frequency components in different context categories of the input image, and the rain patterns can be considered as the common dictionary atoms across different categories. We achieved self-learning of such rain patterns from the input image by utilizing PCA and SVM classifiers, and our experimental results verified that our method produced quantitatively and qualitatively better performance than existing single-image based rain removal methods. Furthermore, in the proposed framework, since image decomposition and self-learning of each context category in the input image can be performed independently, we can deploy a parallel processing architecture in implementation for future speed-up needs.

REFERENCES

[1] K. Garg and S. K. Nayar, "Vision and rain," Int. J. Comput. Vis., vol. 75, no. 1, pp. 3-27, 2007.

[2] K. Garg and S. K. Nayar, "When does a camera see rain?" Proc. IEEE Int. Conf. Comput. Vis., Oct. 2005, pp. 1067-1074.

[3] K. Garg and S. K. Nayar, "Photorealistic rendering of rain streaks," ACM Trans. on Graphics, vol. 25, no. 3, pp. 996-1002, July 2006.

[4] X. Zhang, H. Li, Y. Qi, W. K. Leow, and T. K. Ng, "Rain removal in video by combining temporal and chromatic properties," Proc. IEEE Int. Conf. Multimedia Expo, July 2006, pp. 461–464.

[5] P. C. Barnum, S. Narasimhan, and T. Kanade, "Analysis of rain and snow in frequency space," Int. J. Comput. Vis., vol. 86, no. 2–3, pp. 256–274, 2010.

[6] J. Bossu, N. Hautière, and J. P. Tarel, "Rain or snow detection in image sequences through use of a histogram of orientation of streaks," Int. J. Comput. Vis., vol. 93, no. 3, pp. 348–367, July 2011.

[7] L. W. Kang, C. W. Lin, and Y. H. Fu, "Automatic single-image-based rain streaks removal via image decomposition," IEEE Trans. Image Proc., vol. 21, no. 4, pp. 1742-1755, 2012.

[8] N. Dalal and B. Triggs, "Histograms of oriented gradients for human detection," in Proc. IEEE Conf. Comput. Vis. Pattern Recognit., San Diego, CA, USA, June 2005, pp. 886–893.

[9] L. Itti, C. Koch, and E. Niebur, "A model of saliency-based visual attention for rapid scene analysis," IEEE Trans. Pattern Anal. Mach. Intell., vol. 20, no. 11, pp. 1254–1259, Nov 1998.

[10] J. M. Fadili, J. L. Starck, J. Bobin, and Y. Moudden, "Image decomposition and separation using sparse representations: an overview," Proc. IEEE, vol. 98, no. 6, pp. 983–994, 2010.

[11] C. Tomasi and R. Manduchi, "Bilateral filtering for gray and color images," Proc. IEEE Int. Conf. Comput. Vis., Jan. 1998.

[12] J. Mairal, F. Bach, J. Ponce, and G. Sapiro, "Online learning for matrix factorization and sparse coding," J. Mach. Learn. Res., vol. 11, pp. 19–60, 2010.

[13] M. C. Yang, C. H. Wang, T. Y. Hu, and Y. C. F. Wang, "Learning context-aware sparse representation for single image super-resolution," Proc. IEEE Int. Conf. Image Process., Sept. 2011.

[14] D. Comaniciu and P. Meer, "Mean shift: a robust approach toward feature space analysis," IEEE Trans. Pattern Anal. Mach. Intell., vol. 24, no. 5, pp. 603-619, May 2002.

[15] B. J. Frey and D. Dueck, "Clustering by passing messages between data points," Science, vol. 315, Feb. 2007.

[16] B. Moore, "Principal component analysis in linear systems: controllability, observability, and model reduction," IEEE Trans. Auto. Control, vol. 26, no. 1, pp. 17–32, Feb. 1981.

[17] C. C. Chang and C. J. Lin, "LIBSVM: a library for support vector machines," ACM Trans. Intell. Syst. Technol., vol. 2, no. 3, Article 27, Apr. 2011.

[18] M. Aharon, M. Elad, and A. M. Bruckstein, "The K-SVD: an algorithm for designing of overcomplete dictionaries for sparse representation," IEEE Trans. Signal Process., vol. 54, no. 11, pp. 4311–4322, Nov. 2006.